COMPARISON AMONG FATIGUE LIFE PREDICTION METHODS AND STRESS-STRAIN MODELS UNDER MULTIAXIAL LOADING

Marco Antonio Meggiolaro, meggi@mec.puc-rio.br
Jaime Tupiassú Pinho de Castro, jtcastro@mec.puc-rio.br
Antonio Carlos de Oliveira Miranda, amiranda@tecgraf.puc-rio.br
Pontifical Catholic University of Rio de Janeiro, Rua Marquês de São Vicente 225 Gávea, Rio de Janeiro, RJ, Brazil

Abstract. Principal stress directions may vary when the loading is induced by several independent forces, such as out-of-phase bending and torsion. Uniaxial damage models cannot be reliably applied in this case. Besides the need for multiaxial damage models, another key issue is how to calculate the elastic-plastic stresses from the multiaxial strains. Hooke's law cannot be used to correlate stresses and strains for short lives due to plasticity effects. Ramberg-Osgood cannot be used either to directly correlate principal stresses and strains under multiaxial loading, because this model has been developed for the uniaxial case. The purpose of this work is to critically review and compare a few classical fatigue crack initiation models under multiaxial loading. The studied models include stress-based ones such as Sines, Findley and Dang Van, and strain-based ones such as Brown-Miller, Fatemi-Socie and Smith-Watson-Topper. Modified formulations of the strain-based models are presented to incorporate Findley's idea of using critical planes that maximize damage. To incorporate plasticity effects, four models are studied and compared to correlate stresses and strains under proportional loading: the method of the highest K_t, the constant ratio model, Hoffmann-Seeger's and Dowling's models.

Keywords*: multiaxial fatigue, crack initiation, life prediction models, stress-strain models*

1. INTRODUCTION

Real loads can induce combined bending, torsional, axial and shear stresses, which can generate bi- or tri-axial variable histories at the critical point (in general a notch root), causing the so-called multiaxial fatigue. The load history is said to be proportional when it generates stresses with principal axes with a fixed orientation, while non-proportional loading is associated with principal directions changing in time.

For periodic loads with same frequency, one can also define the concept of in-phase and out-of-phase loading. In-phase loading always leads to proportional histories, however the opposite is not true: e.g., the stresses $\sigma_x = \sigma_I$ and $\sigma_y = \sigma_{II}$ induced on a plate by perpendicular ($\perp$) forces F_x and F_y are always proportional, because the principal axes have a fixed direction even if F_x and F_y are out-of-phase.

On the other hand, out-of-phase axial and torsional stresses always generate non-proportional (NP) loading (Socie and Marquis, 1999). A non-proportionality factor F_{np} of the applied loads can be obtained from the shape of the ellipsis that encloses the history of normal and shear strains, ε and γ. Considering a and b ($b \le a$) as the semi-axes of the ellipsis which encloses the strain path in the Mises diagram $\varepsilon \times \gamma/\sqrt{3}$, then the non-proportionality factor F_{np} is defined as b/a ($0 \le F_{np} \le 1$), see Fig. 1. A further discussion on enclosing ellipses and hyper-ellipsoids is found in (Zouain et al., 2006).

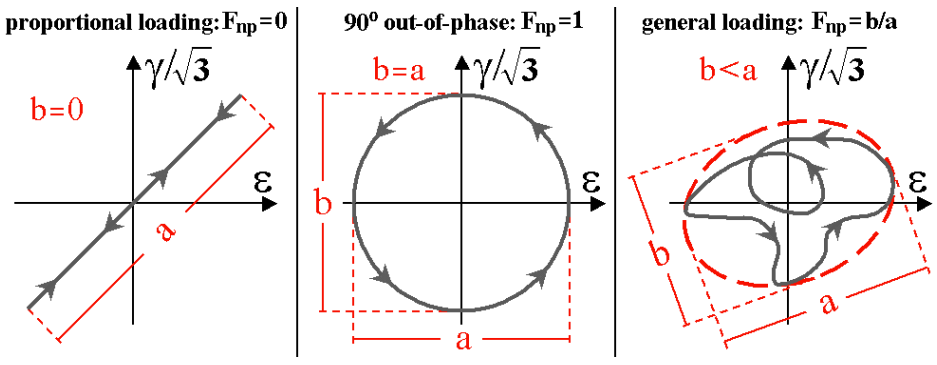

Figure 1. Diagram $\varepsilon \times \gamma/\sqrt{3}$, and associated non-proportionality factors (Socie and Marquis, 1999).

All proportional loadings have shear strains γ proportional to the normal strains ε, with $F_{np} = 0$ and a straight-line trajectory in the $\varepsilon \times \gamma/\sqrt{3}$ diagram. Any loading history with positive F_{np} is NP. Note e.g. that the loading $(\sigma_a \sin\omega t + \tau_a \cos\omega t)$ with $\tau_a = \sigma_a\sqrt{3}/2(1 + \nu)$, caused by traction and torsion 90º out of phase, has $F_{np} = 1$, therefore the maximum possible non-proportionality.

Predictions with NP histories can be very complex, because they involve at least three potential problems:

1. NP hardening: the cyclic hardening coefficient H_c and the ratio $\Delta\sigma/\Delta\varepsilon$ of a few materials increase under NP loading, which significantly decreases the fatigue life of parts subject to a constant $\Delta\varepsilon$;
2. Damage calculation: the SN and εN curves, measured under proportional loading, cannot be directly used when principal directions vary, because in this case the crack propagation plane in general does not match the one from the tests; and
3. Cycle counting: the traditional rain-flow counting techniques cannot be applied to variable amplitude NP loading, because the peaks and valleys of ε in general do not match with the ones of γ, becoming impossible to decide *a priori* which points should be accounted for.

The first two problems will be addressed in this work. A NP hardening model will be presented, to allow for the correct calculation of the equivalent stresses, and multiaxial models based on stress or strain measurements will be used to calculate the damage generated both by proportional and NP loadings.

2. NON-PROPORTIONAL LOADING

A few materials under NP cyclic loading harden much more than it would be predicted from the traditional cyclic $\sigma\varepsilon$ curve. This phenomenon, called NP hardening, depends on the load history (through the NP factor F_{np}) and on the material (through a constant α_{np} of NP hardening, where $0 \le \alpha_{np} \le 1$). The NP hardening can be modeled in general using the same Ramberg-Osgood plastic exponent h_c from the uniaxial cyclic σ-ε curve, and using a new coefficient $H_{cnp} = H_c \cdot (1 + \alpha_{np} \cdot F_{np})$, where H_c is the uniaxial Ramberg-Osgood plastic coefficient. Note that the NP hardening can multiply by up to 2 the value of H_c. The largest NP hardening occurs when $F_{np} = 1$, e.g. under a traction-torsion loading 90^o out of phase which generates a circle in the $\varepsilon \times \gamma/\sqrt{3}$ Mises diagram.

Typically, the NP hardening effect is high in austenitic stainless steels at room temperature ($\alpha_{np} \cong 1$ in the stainless steel 316), medium in carbon steels ($\alpha_{np} \cong 0.3$ in the 1045 steel) and low in aluminum alloys ($\alpha_{np} \cong 0$ for Al 7075). Note that proportional histories do not lead to NP hardening.

The NP hardening happens in materials with low fault stacking energy (which in austenitic stainless steels is only $23 mJ/m^2$) and well spaced dislocations, where the slip bands generated by proportional loading are always planar. In these materials, the NP loads activate crossed slip bands in several directions (due to the rotation of the maximum shear planes), therefore increasing the hardening effect ($\alpha_{np} >> 0$) with respect to the proportional loadings. But in materials with high fault stacking energy (such as aluminum alloys, with typical value of $250 mJ/m^2$) and with close dislocations, the crossed slip bands already happen naturally even under proportional loading, therefore the NP histories do not cause any significant difference in hardening ($\alpha_{np} \cong 0$).

But the Coffin-Manson or the Morrow crack initiation equations cannot account for the influence of NP hardening. This implies that the use of traditional εN equations, which were developed to model uniaxial fatigue problems, can be non-conservative when the loading histories are NP. In the following sections, the multiaxial models to predict NP damage are studied.

3. STRESS-BASED MULTIAXIAL FATIGUE DAMAGE MODELS

It is well known that Tresca or Mises equivalent stresses must be used to predict crack initiation lives, which depend on the cyclic movement of dislocations. However, crack initiation can and should be divided into:

- formation of microcracks, which is almost insensitive to mean stresses and hydrostatic pressure in metals, because it only depends on dislocation movement; followed by
- propagation of the dominant microcrack, which also depends on the crack face opening and the friction between the faces, becoming increasingly sensitive to the applied mean stress σ_m as the microcrack grows.

Microcracks are cracks with dimensions up to the order of the metal grain sizes. Their modeling using classical fracture mechanics is questionable, as opposed to long cracks (typically larger than 1 or 2mm), which have crack propagation rates controlled by ΔK.

However, SN and εN tests bring test specimens to fracture, or to the generation of a small, but easily detectable crack, therefore they include both microcrack initiation and propagation phases. Thus, since the shear stress $\Delta\tau$ controls the initiation of a microcrack, while the normal stress $\sigma_\perp$ perpendicular to its plane (or the hydrostatic stress σ_h, invariant defined as the mean of the normal stresses) controls its opening, both are important to predict the fatigue lives of SN and εN specimens.

In fact, a component under uniaxial traction $\sigma_x = \sigma$ and another under torsion $\tau_{xy} = \sigma/2$ work under the same Tresca equivalent stress, but the microcracks on the plane of τ_{max} in the first component are subject to a normal stress $\sigma_\perp$ perpendicular to that plane that tends to keep their mouth open, exposing the crack tips and decreasing the crack face friction. Therefore, the fatigue damage generated by $\Delta\sigma$ can be greater than the one caused by the torsion $\Delta\tau = \Delta\sigma/2$.

The Mises equivalent stress is able to, at least in part, consider such effect, because the component under torsion would have $\sigma_{Mises} = \tau_{xy}\sqrt{3} = 0.866 \cdot \sigma_x < \sigma$, however σ_{Mises} is insensitive to the hydrostatic stress σ_h. The Mises shear strain τ_{Mises}, which acts on the octahedric planes, does not consider as well the effects of σ_h, relating with σ_{Mises} through:

$$\sigma_{Mises} = \frac{3}{\sqrt{2}}\tau_{Mises} = \frac{1}{\sqrt{2}}\sqrt{(\sigma_1-\sigma_2)^2+(\sigma_1-\sigma_3)^2+(\sigma_2-\sigma_3)^2} \quad (1)$$

Sines (1959) has proposed a fatigue failure criterion under proportional multiaxial stresses, based on $\Delta\tau_{Mises}$ and on $\sigma_{hm} = (\sigma_{xm}+\sigma_{ym}+\sigma_{zm})/3$, the hydrostatic component of the mean stresses (insensitive to the shear stresses):

$$\frac{\Delta\tau_{Mises}}{2} + \alpha_S \cdot (3 \cdot \sigma_{h_m}) = \beta_S \quad (2)$$

where α_S and β_S are adjustable constants for each material, and

$$\Delta\tau_{Mises} = \frac{1}{3}\sqrt{(\Delta\sigma_1-\Delta\sigma_2)^2+(\Delta\sigma_1-\Delta\sigma_3)^2+(\Delta\sigma_2-\Delta\sigma_3)^2} \quad (3)$$

On the other hand, the Findley (1959) criterion, which is also applicable to NP multiaxial loadings, assumes that the crack initiates at the critical plane of the critical point. On the critical plane, the damage caused by the combination $\Delta\tau/2 + \alpha_F \cdot \sigma_\perp$ is maximum, where $\Delta\tau/2$ is the shear stress amplitude on that plane and $\sigma_\perp$ is the normal stress perpendicular to it. Thus, according to Findley the fatigue failure criterion (at the critical plane of the critical point) is

$$\left(\frac{\Delta\tau}{2} + \alpha_F \cdot \sigma_\perp\right)_{max} = \beta_F \quad (4)$$

where α_F and β_F are constants that must be fitted by measurements in at least two types of fatigue tests, e.g., under pure traction and under pure torsion.The critical plane can vary at each i-th event of the NP loads, even when the critical point remains the same, but Findley predicts fatigue failure based on the assumptiom that it ocours in the plane where the sum of the damages associated with $[\Delta\tau_i(\theta)/2 + \alpha_F \cdot \sigma_{\perp i}(\theta)]$ is maximum, where θ is the angle of such plane with respect to a reference direction. The resulting Findley criteria for special cases such as pure torsion and uniaxial traction-compression for a given R-ratio are shown in (Meggiolaro et al., 2007).

From the principle that the damage associated with the initiation of fatigue microcracks cannot be detected from macroscopic measurements, Dang Van (1999) proposed a model that considers the variable micro stresses that act inside a characteristic volume element (VE) of the material, where the macroscopic stresses and strains are supposedly constant. The VE is the unit used in structural analysis to represent the material properties, such as its Young modulus and its several strengths. Thus the VE must be small compared to the component's dimensions, but large compared to the parameter that characterizes the intrinsic anisotropy of the material. For instance, a VE of only $1mm^3$ is sufficient for most structural metal alloys, which have a grain size g (which, being a monocrystal, is intrinsically anisotropic) typically between 10 and 100μm.

The local micro stresses $[\sigma_{ij}]_\mu = \sigma_\mu$ and strains $[\varepsilon_{ij}]_\mu = \varepsilon_\mu$ acting between grains, or between them and small imperfections such as inclusions, e.g., can significantly differ from the macro stresses $[\sigma_{ij}]_M = \sigma_M$ and strains $[\varepsilon_{ij}]_M = \varepsilon_M$, assumed constant in the macroscopic analysis normally used in mechanical design. Therefore, these micro quantities can significantly influence crack initiation. Note that if the term "microscopic" is reserved to the scale associated with interatomic stresses, domain of solid state physics, then its is recommended to use the term "mesoscopic" to describe the intra or intergranular stresses. Thus, the macroscopic stresses reflect the average of the mesoscopic stresses in a VE: $\sigma_M = \int\sigma_\mu dV/V$, where V is the volume of the VE. Similarly, $\varepsilon_M = \int\varepsilon_\mu dV/V$.

The macroscopic stresses and strains are assumed constant at the characteristic volume element VE of the material, however the mesoscopic intergranular stresses can vary a lot within the VE, influencing crack initiation.

Since the microcracks initiate at persistent slip bands, Dang Van assumed that fatigue damage was caused by the mesoscopic shear strain history $\tau_\mu(t)$ and influenced by the mesoscopic hydrostatic stress history $\sigma_{\mu h}(t)$. The simplest failure criterion involving these components is the linear combination given by:

$$\tau_\mu(t) + \alpha_{DV} \cdot \sigma_{\mu h}(t) = \beta_{DV} \quad (5)$$

Other similar criteria can be found in (Socie and Marquis, 1999) and (Gonçalves et al., 2005).

4. STRAIN-BASED MULTIAXIAL FATIGUE DAMAGE MODELS

The three multiaxial failure criteria presented above are based on macroscopic stresses that are supposedly elastic, therefore they are only applicable when σ_{Mises} is much smaller than the cyclic yielding strength S_{yc}. Thus, as in the case of the SN method, they can only be used to predict very long fatigue lives.

Otherwise, it is imperative to use fatigue damage criteria based on applied strains instead of stresses (Socie and Marquis, 1999), using the principles studied in the so-called εN method.

One of the simplest models is the one based on the γN curve, similar to Coffin-Manson's equation, which uses the largest shear strain range $\Delta\gamma_{max}$ acting on the specimen ($\gamma_{ij} \equiv 2\varepsilon_{ij}$, $i \neq j$) to predict fatigue life

$$\frac{\Delta\gamma_{max}}{2} = \frac{\tau_c}{G}(2N)^{b_\gamma} + \gamma_c(2N)^{c_\gamma} \tag{6}$$

where τ_c, b_γ, γ_c and c_γ are parameters similar to the ones from Coffin-Manson, $G = E/[2(1 + \nu)]$ is the shear modulus, ν being Poisson's coefficient. If no experimental data is available, the γN curve can at least in principle be estimated assuming $\tau_c \cong \sigma_c/\sqrt{3}$, $b_\gamma \cong b$, $\gamma_c \cong \varepsilon_c\sqrt{3}$ and $c_\gamma \cong c$.

The γN curve is only recommended to model fatigue damage in materials that are more sensitive to shear strains (which have small α in the Mohr models, see Meggiolaro et al., 2007), if the mean loads are zero. It would be expected that such materials would have a shorter torsional fatigue life than similar materials more sensitive to normal stresses.

The Brown-Miller (1973) model can consider the mean stress effects, combining the maximum range of the shear strain $\Delta\gamma_{max}$ to the range of normal strain $\Delta\varepsilon_\perp$ (through the term $\Delta\gamma_{max}/2 + \alpha_{BM}\cdot\Delta\varepsilon_\perp$) and the mean normal stress $\sigma_{\perp m}$ perpendicular to the plane of maximum shear strain, to obtain the fatigue life N:

$$\frac{\Delta\gamma_{max}}{2} + \alpha_{BM}\cdot\Delta\varepsilon_\perp = \beta_1\frac{\sigma_c - 2\sigma_{\perp m}}{E}(2N)^b + \beta_2\varepsilon_c(2N)^c \tag{7}$$

where α_{BM} is a fitting parameter ($\alpha_{BM} \cong 0.3$ for ductile metals in lives near the fatigue limit), $\beta_1 = (1 + \nu) + (1 - \nu)\cdot\alpha_{BM}$, and $\beta_2 = 1.5 + 0.5\cdot\alpha_{BM}$.

This equation was adapted from Morrow mean load εN model to fit uniaxial traction test data, where the mean stress σ_m is equal to $2\sigma_{\perp m}$ (because $\sigma_{\perp m}$ acts perpendicularly to the plane of γ_{max}, therefore it is worth half of σ_m).

The values of β_1 and β_2 are obtained assuming uniaxial traction:

$$\left.\begin{aligned}\Delta\gamma_{max} &= (1+\nu)\Delta\varepsilon \\ \Delta\varepsilon_\perp &= (1-\nu)\Delta\varepsilon/2\end{aligned}\right\} \Rightarrow \frac{\Delta\gamma_{max}}{2} + \alpha_{BM}\Delta\varepsilon_\perp = \frac{\Delta\varepsilon}{2}[(1+\nu) + \alpha_{BM}(1-\nu)] \tag{8}$$

From Eq. (8), the coefficients $\beta_1 = (1 + \nu) + (1 - \nu)\cdot\alpha_{BM}$ and $\beta_2 = 1.5 + 0.5\cdot\alpha_{BM}$ are obtained, because $\nu = 0.5$ for plastic strains, which preserve volume. The original Brown-Miller model assumes that the elastic strains have $\nu = 0.3$, therefore $\beta_1 \cong (1 + 0.3) + (1 - 0.3)\cdot\alpha_{BM} = 1.3 + 0.7\cdot\alpha_{BM}$.

The Brown-Miller model is frequently used in multiaxial fatigue, even though it is not reasonable to assume that $\Delta\varepsilon_\perp$ can control the opening and closure of microcracks, because the range $\Delta\varepsilon$ does not include information about maximum stresses or strains. E.g., two microcracks with the same $\Delta\gamma_{max}$ and $\Delta\varepsilon_\perp$ can have very different fatigue lives if one is opened (under traction) and the other is closed (under compression) due to the mean load effect. The use of $\sigma_{\perp m}$ compensates in part for this model flaw, however the mean stress effect is only considered in the elastic part.

Fatemi and Socie (1988) suggested replacing $\Delta\varepsilon_\perp$ by the maximum normal stress $\sigma_{\perp max}$ perpendicular to the plane of maximum shear strain, applying it to the γN curve:

$$\frac{\Delta\gamma_{max}}{2}\left(1 + \alpha_{FS}\frac{\sigma_{\perp max}}{S_{yc}}\right) = \frac{\tau_c}{G}(2N)^{b_\gamma} + \gamma_c(2N)^{c_\gamma} \tag{9}$$

Note that the value of α_{BM} and α_{FS} indicates whether the material is more sensitive to τ (α_{BM} or $\alpha_{FS} << 1$) or to σ (α_{BM} or $\alpha_{FS} >> 1$).

If the propagation phase of the microcracks (more sensitive to σ) is dominant over initiation, the Smith-Watson-Topper (SWT) multiaxial model can be used (Smith et al., 1970):

$$\frac{\Delta\varepsilon_1}{2}\cdot\sigma_{\perp 1 max} = \frac{\sigma_c^2}{E}(2N)^{2b} + \sigma_c\varepsilon_c(2N)^{b+c} \tag{10}$$

where $\Delta\varepsilon_1$ is the range of the maximum principal strain and $\sigma_{\perp 1 max}$ is the stress peak in the direction perpendicular to ε_1.

Figure 2 summarizes the parameters used in the above strain-based models. In addition, there are several other models based on the plastic energy dissipated by the hysteresis loops, and other combining energy with critical planes, see (Socie and Marquis, 1999).

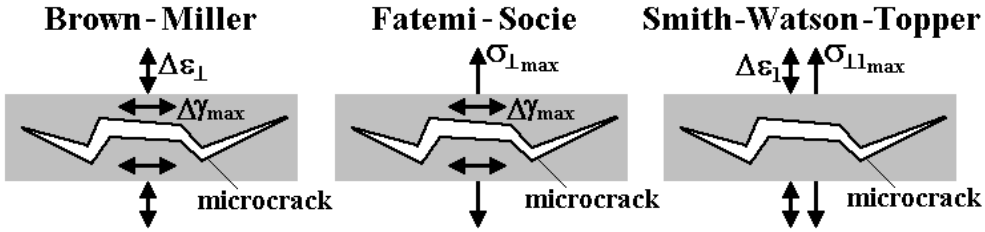

Figure 2. Parameters which affect the strain-based multiaxial models.

It is important to note that the plane of maximum shear strain amplitude $\Delta\gamma_{max}/2$ (used in Brown-Miller's and Fatemi-Socie's models) is in general different from the planes that would maximize the respective damage parameters ($\Delta\gamma/2 + \alpha_{BM}\cdot\Delta\varepsilon_\perp$ for Brown-Miller, and $\Delta\gamma\cdot(1 + \alpha_{FS}\cdot\sigma_{\perp max}/S_{yc})/2$ for Fatemi-Socie). But if these are the parameters that cause damage, it is reasonable to argue that fatigue life should be calculated on the critical plane that maximizes them (in a similar way as done in Findley's model), and not on the plane of $\Delta\gamma_{max}$. In this way, it is a good idea to modify the Brown-Miller and Fatemi-Socie models introducing subtle but important changes:

$$\frac{\Delta\gamma_{max}}{2} + \alpha_{BM}\cdot\Delta\varepsilon_\perp \Rightarrow \left(\frac{\Delta\gamma}{2} + \alpha_{BM}\cdot\Delta\varepsilon_\perp\right)_{max} \quad \text{and} \quad \frac{\Delta\gamma_{max}}{2}\left(1 + \alpha_{FS}\frac{\sigma_{\perp max}}{S_{yc}}\right) \Rightarrow \left(\frac{\Delta\gamma}{2} + \alpha_{FS}\frac{\Delta\gamma}{2}\frac{\sigma_{\perp\gamma}}{S_{yc}}\right)_{max} \tag{11}$$

The use of critical planes that maximize the damage parameters in each model has the advantage of predicting not only the fatigue life but also the dominant planes where the crack will initiate. However, these calculations are not simple and require the use of sofisticated numerical methods.

This idea can also be applied to the SWT model, calculating the critical plane where the product between the normal strain range $\Delta\varepsilon_\perp$ and the normal stress peak $\sigma_{\perp max}$ is maximized, adopting the modification

$$\frac{\Delta\varepsilon_1}{2}\cdot\sigma_{\perp 1_{max}} \Rightarrow \left(\frac{\Delta\varepsilon_\perp}{2}\cdot\sigma_{\perp_{max}}\right)_{max} \tag{12}$$

A great advantage of the Fatemi-Socie (or SWT) model is to be able to consider the effect of NP hardening from the peak of normal stress $\sigma_{\perp max}$ (or $\sigma_{\perp 1max}$). In stainless steels, e.g., a NP history leads to a much higher damage than a proportional one with the same $\Delta\gamma_{max}$ and $\Delta\varepsilon_\perp$, because the NP hardening increases the value of $\sigma_{\perp max}$ (or $\sigma_{\perp 1max}$). Note that Brown-Miller would wrongfully predict the same damage in both histories (because $\Delta\gamma_{max}$ and $\Delta\varepsilon_\perp$ would be the same), and only the Fatemi-Socie and SWT models would be able to correctly account for the greater damage of the NP loading (assuming that H_{cnp} would be used to obtain $\sigma_{\perp max}$ and $\sigma_{\perp 1max}$).

5. MULTIAXIAL STRESS-STRAIN RELATIONS

Hooke's law cannot be used to correlate stresses and strains for short multiaxial fatigue life predictions, due to plasticity effects. The hookean stresses and strains, $\tilde{\sigma}$ and $\tilde{\varepsilon}$, defined as the values of σ and ε obtained assuming that the material would be linear elastic (using Hooke's law and, at the notches, considering elastic stress K_σ and strain K_ε concentration factors), can only be applied for long life predictions.

In addition, Ramberg-Osgood cannot be used either to directly correlate principal stresses and strains σ_i and ε_i (i = 1, 2, 3) of a multiaxial history, because this model has been developed for the uniaxial case.

However, if the elastic nominal stress range $\Delta\sigma_n$ is caused by in-phase loading, then it is trivial to calculate the elastic-plastic stresses and strains at the notch root using the "highest K_t method". In this approximate method, the equivalent nominal stress range $\Delta\sigma_n$ calculated from Tresca or Mises is used to obtain $\Delta\sigma$ and $\Delta\varepsilon$ at the notch root using Ramberg-Osgood and (for safety, because the method is conservative) the highest K_t in Neuber's rule. Remember that the multiaxial loadings can result, at the same notch root, in different values of K_t for traction, bending, torsion and shear loadings, but only the maximum one is used. To generate more accurate predictions for notches under combined stresses, it is recommended to use multiaxial σ-ε relations.

Several models have been proposed to correlate σ_i and ε_i in proportional histories, e.g.: the constant ratio model (Socie and Marquis, 1999), Hoffmann-Seeger's model (Hoffmann and Seeger, 1985), and Dowling's model (Dowling et al., 1977). To present these three models, it is necessary to define a few variables involved in their formulation:

- $\tilde{\sigma}_1$, $\tilde{\sigma}_2$, $\tilde{\sigma}_3$, $\tilde{\varepsilon}_1$, $\tilde{\varepsilon}_2$, $\tilde{\varepsilon}_3$: hookean principal stresses and strains at the notch root (elastically calculated using Hooke's law and elastic K_σ and K_ε);
- $\tilde{\sigma}_{Mises}$, $\tilde{\varepsilon}_{Mises}$: hookean Mises stress and strain (at the notch root), calculated using the above variables;
- σ_1, σ_2, σ_3, ε_1, ε_2, ε_3: elastic-plastic principal stresses and strains (notch root);
- σ_{Mises}, ε_{Mises}: Mises stress and strain (notch root);
- λ_2, λ_3: ratios between pairs of principal stresses, where $\lambda_2 = \sigma_2/\sigma_1$ and $\lambda_3 = \sigma_3/\sigma_1$, both between –1 and 1;
- ϕ_2, ϕ_3: ratios between pairs of principal strains, where $\phi_2 = \varepsilon_2/\varepsilon_1$, $\phi_3 = \varepsilon_3/\varepsilon_1$, both between –1 and 1; and
- λ_{Mises}, ϕ_{Mises}: Mises ratios $\lambda_{Mises} = \sigma_{Mises}/\sigma_1$ and $\phi_{Mises} = \varepsilon_{Mises}/\varepsilon_1$.

From the above definitions, it is possible to obtain

$$\lambda_{Mises} = \frac{\sigma_{Mises}}{\sigma_1} = \frac{1}{\sqrt{2}}\sqrt{(1-\lambda_2)^2 + (1-\lambda_3)^2 + (\lambda_2-\lambda_3)^2} \tag{13}$$

$$\phi_{Mises} = \frac{\varepsilon_{Mises}}{\varepsilon_1} = \frac{1}{\sqrt{2}(1+\nu)}\sqrt{(1-\phi_2)^2 + (1-\phi_3)^2 + (\phi_2-\phi_3)^2} \tag{14}$$

The three models are described next.

5.1. Constant Ratio Model

The *constant ratio model* (Socie and Marquis, 1999) assumes that, under a proportional history, the bi-axial ratios λ_2, λ_3, ϕ_2 and ϕ_3 remain constant even after yielding has occurred. Since the elastic Poisson coefficient ν_{el} is typically between 1/4 and 1/3 in most metal alloys, significantly different than the plastic $\nu_{pl} = 0.5$, these ratios are in fact not constant, but for small plastic strains this is a good approximation. These ratios can be estimated from the elastic stresses and strains, obtained from Hooke's law using elastic K_σ and K_ε:

$$\lambda_2 \cong \frac{\tilde{\sigma}_2}{\tilde{\sigma}_1},\ \lambda_3 \cong \frac{\tilde{\sigma}_3}{\tilde{\sigma}_1},\ \phi_2 \cong \frac{\tilde{\varepsilon}_2}{\tilde{\varepsilon}_1},\ \phi_3 \cong \frac{\tilde{\varepsilon}_3}{\tilde{\varepsilon}_1} \tag{15}$$

Therefore, λ_{Mises} is also a constant, leading to

$$\lambda_{Mises} \cong \frac{\tilde{\sigma}_{Mises}}{\tilde{\sigma}_1} \Rightarrow \tilde{\sigma}_{Mises} \cong \frac{\tilde{\sigma}_1}{\sqrt{2}}\sqrt{(1-\lambda_2)^2 + (1-\lambda_3)^2 + (\lambda_2-\lambda_3)^2} \tag{16}$$

and, similarly, ϕ_{Mises} can be calculated from ϕ_2 and ϕ_3. The cyclic σ-ε relation is then defined using Mises and the Ramberg-Osgood uniaxial parameters

$$\varepsilon_{Mises} = \frac{\sigma_{Mises}}{E} + \left(\frac{\sigma_{Mises}}{H_c}\right)^{1/h_c} \tag{17}$$

If no notches are present, then the above equation is used together with the estimates for λ_{Mises}, ϕ_{Mises}, λ_2, λ_3, ϕ_2 and ϕ_3 to obtain σ_i from ε_i (i = 1, 2, 3), or vice-versa. In notched components, $\tilde{\sigma}_{Mises}$ (elastically calculated including the K_fs) is applied to a variation of Neuber's rule to calculate the elastic-plastic σ_{Mises} and ε_{Mises}, σ_i and ε_i (i = 1, 2, 3):

$$\frac{(\tilde{\sigma}_{Mises})^2}{E} = \sigma_{Mises}\cdot\varepsilon_{Mises} = \frac{(\sigma_{Mises})^2}{E} + \sigma_{Mises}\cdot\left(\frac{\sigma_{Mises}}{H_c}\right)^{1/h_c} \tag{18}$$

After calculating σ_{Mises} and ε_{Mises}, the constant ratio model obtains the principal stress and strain using:

$$\begin{cases} \sigma_1 = \sigma_{Mises}/\lambda_{Mises},\ \sigma_2 = \lambda_2\sigma_1,\ \sigma_3 = \lambda_3\sigma_1 \\ \varepsilon_1 = \varepsilon_{Mises}/\phi_{Mises},\ \varepsilon_2 = \phi_2\varepsilon_1,\ \varepsilon_3 = \phi_3\varepsilon_1 \end{cases} \tag{19}$$

5.2. Hoffmann-Seeger's Model

Hoffmann-Seeger's model (Hoffmann and Seeger, 1985) uses the same cyclic σ-ε relation and the same variation of Neuber's rule presented above to calculate σ_{Mises} and ε_{Mises}, but it assumes that:

- the critical point happens at the surface, with principal stresses σ_1 and σ_2;
- σ_3 is defined normal to the surface, therefore $\sigma_3 = 0$ (and then $\lambda_3 = 0$); and
- only the ratio $\phi_2 = \tilde{\varepsilon}_2 / \tilde{\varepsilon}_1$ is estimated using the linear elastic (hookean) values.

After calculating σ_{Mises} and ε_{Mises}, σ_i and ε_i are estimated from:

$$\begin{cases} \sigma_1 = \sigma_{Mises} / \bar{\lambda}_{Mises}, \ \sigma_2 = \bar{\lambda}_2 \sigma_1, \ \sigma_3 = 0 \\ \varepsilon_1 = \dfrac{(1 - \bar{\lambda}_2 \bar{\nu}) \varepsilon_{Mises}}{\bar{\lambda}_{Mises}}, \ \varepsilon_2 = \phi_2 \varepsilon_1, \ \varepsilon_3 = -\bar{\nu} \varepsilon_1 \dfrac{1 + \bar{\lambda}_2}{1 - \bar{\lambda}_2 \bar{\nu}} \end{cases} \tag{20}$$

$$\bar{\nu} = \frac{1}{2} - \frac{(1/2 - \nu_{el}) \sigma_{Mises}}{E \cdot \varepsilon_{Mises}}, \ \bar{\lambda}_2 = \frac{\phi_2 + \bar{\nu}}{1 + \phi_2 \bar{\nu}}, \ \bar{\lambda}_{Mises} = \sqrt{1 - \bar{\lambda}_2 + \bar{\lambda}_2^2} \tag{21}$$

5.3. Dowling's Model

The model proposed in (Dowling et al., 1977) also assumes that the principal stresses σ_1 and σ_2 act on the surface of the critical point (therefore σ_3 is zero), and it considers λ_2 and ϕ_2 constant, estimating them from their hookean values

$$\lambda_2 = \frac{\sigma_2}{\sigma_1} \cong \frac{\tilde{\sigma}_2}{\tilde{\sigma}_1} \cong \frac{\phi_2 + \nu}{1 + \phi_2 \nu}, \quad \phi_2 = \frac{\varepsilon_2}{\varepsilon_1} \cong \frac{\tilde{\varepsilon}_2}{\tilde{\varepsilon}_1} \cong \frac{\lambda_2 - \nu}{1 - \lambda_2 \nu} \tag{22}$$

Exceptionally, σ_2 is defined here as the lowest principal stress at the surface, even if σ_2 is smaller than σ_3 (i.e. the convention $\sigma_3 \le \sigma_2 \le \sigma_1$ is violated if $\lambda_2 < 0$).

The greatest difference between the previous two models and Dowling's is that the latter correlates σ_1 and ε_1 directly using effective Ramberg-Osgood parameters E^* and H_c^*

$$\varepsilon_1 = \frac{\sigma_1}{E^*} + \left(\frac{\sigma_1}{H_c^*}\right)^{1/h_c} \text{, where } E^* = \left(\frac{1 + \phi_2 \nu}{1 - \nu^2}\right) \cdot E \ , \ H_c^* = H_c \cdot \left(\frac{2}{2 - \lambda_2}\right)^{h_c} (1 - \lambda_2 + \lambda_2^2)^{0.5(h_c - 1)} \tag{23}$$

In notched components, another variation of Neuber's rule must be used to calculate σ_1 (and then ε_1) from $\tilde{\sigma}_{Mises}$:

$$\frac{(\tilde{\sigma}_{Mises})^2}{E} = \sigma_1 \cdot \varepsilon_1 = \frac{\sigma_1^2}{E^*} + \sigma_1 \cdot \left(\frac{\sigma_1}{H_c^*}\right)^{1/h_c} \tag{24}$$

The other principal stresses and strains are obtained from σ_1 and ε_1:

$$\sigma_2 = \lambda_2 \sigma_1, \ \sigma_3 = 0, \ \varepsilon_2 = \phi_2 \varepsilon_1, \ \varepsilon_3 = -\bar{\nu} \varepsilon_1 \frac{1 + \lambda_2}{1 - \lambda_2 \bar{\nu}}, \ \bar{\nu} = \frac{1}{2} - \left(\frac{1}{2} - \nu\right) \frac{\sigma_1}{E^* \varepsilon_1} \tag{25}$$

The largest shear strain γ_{max} can then be calculated from the maximum difference between the principal strains ε_i (i = 1, 2, 3), obtaining not only its magnitude but also the plane where this maximum occurs.

It is important to note that the three presented models (formulated using the cyclic σ-ε curve) can also be applied to the hysteresis loops equations, by replacing in each equation ε with Δε/2 and also σ with Δσ/2. The presented models are compared next.

6. COMPARISON AMONG THE MULTIAXIAL MODELS

The presented multiaxial models are compared considering a notched 1020 steel shaft with diameter *d* equal to 60mm under alternate bending moment M_a of 2kNm and torsion T_a of 3kNm, in phase, with stress concentration factors in bending K_{tM} equal to 3.4 and in torsion K_{tT} equal to 2.4.

Assuming the alternate nominal stress σ_{na} as elastic, then $\sigma_{n_a}=\sqrt{(32M_a)^2+3(16T_a)^2}\,/\,\pi d^3=155MPa$. This stress is lower than the cyclic yielding strength S_{yc} = 241MPa, therefore the hypothesis of σ_{na} elastic is valid.

Using the "highest K_t method" through the highest K_t = 3.4, σ_a and ε_a are calculated using Mises and Neuber

$$(K_t\sigma_{n_a})^2=(3.4\cdot 155)^2=\sigma_a\varepsilon_a E=\sigma_a{}^2+203000\cdot\sigma_a\left(\frac{\sigma_a}{772}\right)^{1/0.18}\Rightarrow\begin{cases}\sigma_a=279MPa\\ \varepsilon_a=0.49\%\end{cases} \tag{26}$$

and then the life N of the shaft is

$$\frac{\Delta\varepsilon}{2}=\varepsilon_a=\frac{896}{203000}(2N)^{-0.12}+0.41(2N)^{-0.51}\Rightarrow N=5871\ cycles \tag{27}$$

To use the multiaxial stress-strain models, the hookean stresses at the notch root are calculated considering K_{tM} = 3.4 and K_{tT} = 2.4 as purely elastic:

$$\tilde{\sigma}_{a_{Mises}}=\sqrt{\left(K_{tM}\sigma_M\right)^2+3\left(K_{tT}\tau_T\right)^2}=\frac{\sqrt{(3.4\cdot 32\cdot M_a)^2+3(2.4\cdot 16\cdot T_a)^2}}{\pi(0.060)^3} \tag{28}$$

$$\tilde{\sigma}_{a_{1,2}}=\frac{K_{tM}\sigma_M}{2}\pm\sqrt{\left(\frac{K_{tM}\sigma_M}{2}\right)^2+\left(K_{tT}\tau_T\right)^2}=160\pm 234MPa \tag{29}$$

Thus, the hookean stresses are $\tilde{\sigma}_{a_{Mises}}$ = 435MPa, $\tilde{\sigma}_{a_1}$ = 394MPa, $\tilde{\sigma}_{a_2}$ = –73MPa and $\tilde{\sigma}_{a_3}$ = 0, which can be correlated to the principal hookean strains from Hooke's law (considering ν = 0.3):

$$\tilde{\varepsilon}_{a_1}=0.205\%,\ \tilde{\varepsilon}_{a_2}=-0.094\%,\ \tilde{\varepsilon}_{a_3}=-0.047\%,\ \tilde{\varepsilon}_{a_{Mises}}=0.214\% \tag{30}$$

From the constant ratio and Hoffmann-Seeger models,

$$\frac{\tilde{\sigma}_{a_{Mises}}{}^2}{E}=0.93=\frac{\sigma_{a_{Mises}}{}^2}{E}+\sigma_{a_{Mises}}\cdot\left(\frac{\sigma_{a_{Mises}}}{772}\right)^{1/0.18}\Rightarrow\sigma_{a_{Mises}}=259\,MPa \tag{31}$$

$$\varepsilon_{a_{Mises}}=\frac{\sigma_{a_{Mises}}}{203000}+\left(\frac{\sigma_{a_{Mises}}}{772}\right)^{1/0.18}\Rightarrow\varepsilon_{a_{Mises}}=0.360\% \tag{32}$$

From the constant ratio model, the hookean stresses and strains are used to estimate λ_{Mises} = 1.105, λ_2 = –0.185, λ_3 = 0, ϕ_{Mises} = 1.046, ϕ_2 = –0.460 and ϕ_3 = –0.231, so the alternate principal stresses and strains are

$$\begin{aligned}&\sigma_{a_1}=259/1.1=235MPa,\ \sigma_{a_2}=\lambda_2\sigma_{a_1}=-44MPa,\ \sigma_{a_3}=0\\ &\varepsilon_{a_1}=0.359\%/1.046=0.344\%,\ \varepsilon_{a_2}=\phi_2\varepsilon_{a_1}=-0.158\%,\ \varepsilon_{a_3}=\phi_3\varepsilon_{a_1}=-0.080\%\end{aligned} \tag{33}$$

On the other hand, Hoffmann-Seeger's model predicts

$$\begin{aligned}&\bar{\nu}=\frac{1}{2}-\left(\frac{1}{2}-\nu\right)\frac{\sigma_{a_{Mises}}}{E\cdot\varepsilon_{a_{Mises}}}=0.5-0.2\frac{259}{203000\cdot 0.00359}=0.429\\ &\bar{\lambda}_2=\frac{\phi_2+\bar{\nu}}{1+\phi_2\bar{\nu}}=\frac{-0.46+\bar{\nu}}{1-0.46\bar{\nu}}=-0.0387,\ \bar{\lambda}_{Mises}=\sqrt{1-\bar{\lambda}_2+\bar{\lambda}_2{}^2}=1.02\end{aligned} \tag{34}$$

resulting in alternate principal stresses and strains

$$\begin{cases}\sigma_{a_1}=259/1.02=254MPa,\ \sigma_{a_2}=-0.0387\cdot\sigma_{a_1}=-10MPa,\ \sigma_{a_3}=0\\ \varepsilon_{a_1}=(1-\bar{\lambda}_2\bar{\nu})0.360\%/1.02=0.359\%,\ \varepsilon_{a_2}=\phi_2\varepsilon_{a_1}=-0.165\%\\ \varepsilon_{a_3}=-\bar{\nu}\varepsilon_{a_1}(1+\bar{\lambda}_2)/(1-\bar{\lambda}_2\bar{\nu})=-0.146\%\end{cases} \tag{35}$$

Dowling's model uses the elastic ratios $\lambda_2 = -0.185$ and $\phi_2 = -0.460$ to calculate the effective parameters of the hardening curve, $E^*=192GPa$ and $H_c^*=700MPa$, resulting in

$$\frac{(\tilde{\sigma}_{a_{Mises}})^2}{E}=0.93=\sigma_{a_1}\cdot\varepsilon_{a_1}=\frac{\sigma_{a_1}^2}{E^*}+\sigma_{a_1}\cdot\left(\frac{\sigma_{a_1}}{H_c^*}\right)^{1/h_c}\Rightarrow\begin{cases}\sigma_{a1}=240MPa\\ \varepsilon_{a1}=0.388\%\end{cases} \tag{36}$$

$$\sigma_{a_2}=\lambda_2\sigma_{a_1}=-45MPa,\ \sigma_{a_3}=0,\ \varepsilon_{a_2}=\phi_2\varepsilon_{a_1}=-0.179\%,\ \varepsilon_{a_3}=-\bar{\nu}\varepsilon_{a_1}\frac{1+\lambda_2}{1-\lambda_2\bar{\nu}}=-0.127\%\ (\bar{\nu}=0.436) \tag{37}$$

For all considered models, the maximum shear strain amplitude is calculated from $\gamma_{amax} = \varepsilon_{a1} - \varepsilon_{a2}$, assuming that the directions 1 and 2 are respectively the ones with maximum and minimum principal strains. The maximum normal strains and stresses in the plane of γ_{amax} are

$$\varepsilon_{a\perp} = (\varepsilon_{a1} + \varepsilon_{a2})/2 \quad \text{and} \quad \sigma_{a\perp} = (\sigma_{a1} + \sigma_{a2})/2 \tag{38}$$

Since in this problem the mean stresses and strains are zero, the values used by the Brown-Miller, Fatemi-Socie and SWT strain-life models are respectively $\Delta\varepsilon_\perp = 2\varepsilon_{a\perp}$, $\sigma_{\perp max} = \sigma_{a\perp}$ and $\sigma_{\perp 1max} = \sigma_{a1}$.

Table 1 summarizes the stresses and strains obtained from the hookean values (obtained assuming elastic stresses, which must not be used in life predictions in the presence of significant plasticity), from the "highest K_t method", and from the three presented multiaxial stress-strain models: the constant ratio, Hoffmann-Seeger's and Dowling's.

Table 1. Stresses (in MPa) and strains predicted from the studied models.

	hookean values	highest K_t method	constant ratio	Hoffman-Seeger	Dowling
$\sigma_{a_{Mises}}$	435	279	259	259	265
$\varepsilon_{a_{Mises}}$	0.214%	0.488%	0.360%	0.360%	0.418%
σ_{a_1}	394	253	235	254	240
σ_{a_2}	−73	−47	−44	−10	−45
σ_{a_3}	0	0	0	0	0
ε_{a_1}	0.205%	0.466%	0.344%	0.359%	0.388%
ε_{a_2}	−0.094%	−0.215%	−0.158%	−0.165%	−0.179%
ε_{a_3}	−0.047%	−0.108%	−0.080%	−0.146%	−0.127%
$\gamma_{a_{max}}$	0.299%	0.681%	0.502%	0.524%	0.567%
$\Delta\varepsilon_\perp$	0.111%	0.251%	0.186%	0.194%	0.209%
$\sigma_{\perp_{max}}$	160	103	95	122	98

Note from Tab. 1 that the "highest K_t method" is conservative, especially for the calculated strains, but not too much, therefore it could be used in practice. The three multiaxial models are in theory more accurate, predicting approximately the same values.

Now, using the above results, the fatigue life N can be obtained from the several damage models.

Considering the εN curve, the Mises strain ε_{aMises} can be used to calculate N. If, instead of the εN curve, the γN curve is considered, estimating its coefficients from $\tau_c \cong \sigma_c/\sqrt{3}$, $b_\gamma \cong b$, $\gamma_c \cong \varepsilon_c\sqrt{3}$ and $c_\gamma \cong c$, then γ_{amax} is used. Considering Brown-Miller's model, with its constants estimated from $\alpha_{BM} \cong 0.3$, $\beta_1 = 1.3 + 0.7\cdot\alpha_{BM} = 1.51$ and $\beta_2 = 1.5 + 0.5\cdot\alpha_{BM} = 1.65$, then $\Delta\varepsilon_\perp$ is the needed parameter. Fatemi-Socie's model can also be used, estimating $\alpha_{FS} \cong S_{yc}/\sigma_c = 241MPa/896MPa \cong 0.27$ and the γN curve above. And, finally, considering SWT's model, uses $\Delta\varepsilon_1/2 = \varepsilon_{a1}$ and, since the mean loads are zero, $\sigma_{\perp 1max} = \sigma_{a1}$ to obtain the fatigue life. These calculations are performed considering each of the columns of Tab. 1. The results are shown in Tab. 2.

Except from the results obtained from the hookean values (which are significantly non-conservative), all combinations of multiaxial damage models with multiaxial stress-strain relations resulted in similar lives, varying between 5900 and 20300 cycles. Therefore, it is reasonable to consider in proportional histories the use of simplifications such as the "highest K_t method" and the εN curve applied to $\Delta\varepsilon_{Mises}/2$, despite the conservative predictions.

Table 2. Fatigue lives (in cycles) predicted from the studied multiaxial models.

	Mises + εN curve	γN curve	Brown-Miller	Fatemi-Socie	SWT
hookean values	59500	94300	63000	56200	18300
highest K_t method	5900	9120	6440	6940	8470
constant ratio	13000	20300	14100	15500	18300
Hoffmann-Seeger	13000	18100	12600	12900	14200
Dowling	8770	14700	10300	11200	13600

The hookean values result in poor estimates, overestimating σ_{a1} and underestimating ε_{a1}, but it interestingly estimates quite well the product $\sigma_{a1}\varepsilon_{a1}$ (because, according to Neuber, $\tilde{\sigma}_{a_1}\tilde{\varepsilon}_{a_1} \cong \sigma_{a_1}\varepsilon_{a_1}$), therefore they resulted in good predictions when combined with SWT's model, based on this product. But in NP histories, the NP hardening can have a significant effect in the fatigue life. In addition, none of the presented σ-ε models is valid in the NP case (because they assumed ϕ_2 constant). In the NP case, incremental plasticity models must be used (Socie and Marquis, 1999).

7. CONCLUSIONS

In this work, the multiaxial damage models of Sines, Findley and Dang Van, applicable to long fatigue lives, and Brown-Miller, Fatemi-Socie and Smith-Watson-Topper (SWT), which consider plasticity, were reviewed. Among the strain-based models, Fatemi-Socie's and SWT's can consider the effects of NP hardening. In order to generate more realistic models, it is important to modify these criteria to calculate fatigue life in the critical plane where the damage parameters of each model are maximized. The main multiaxial stress-strain models were also reviewed and compared. The analysis showed that multiaxial stress-strain relations must be used instead of uniaxial ones, even though a few simplifications are adequate, such as the "highest K_t method" for notched components. Since the critical point of a structure is usually in its surface, in general a 2D analysis (under plane stress) is enough for multiaxial fatigue design. The best predictions should be the ones from multiaxial models that use the critical plane idea, where the damage parameters are maximized.

8. REFERENCES

Brown, M. and Miller, K.J., 1973, "A Theory for Fatigue Under Multiaxial Stress-Strain Conditions", Institute of Mech. Engineers, Vol.187, pp. 745-756.

Dang Van, K. and Papadopoulos, I.V., 1999, "High-Cycle Metal Fatigue", Springer.

Dowling, N.E., Brose, W.R. and Wilson, W.K., 1977, "Notched Member Fatigue Life Predictions by the Local Strain Approach", in Fatigue Under Complex Loading: Analysis and Experiments, AE-6, SAE.

Fatemi, A. and Socie, D.F., 1988, "A Critical Plane Approach to Multiaxial Damage Including Out-of-Phase Loading", Fatigue and Fracture of Eng. Materials and Structures, Vol.11, No. 3, pp.149-166.

Findley, W.N., 1959, "A Theory for the Effect of Mean Stress on Fatigue of Metals Under Combined Torsion and Axial Load or Bending", Journal of Engineering for Industry, pp.301-306.

Gonçalves, C.A., Araújo, J.A. and Mamiya, E.N., 2005, "Multiaxial fatigue: a stress based criterion for hard metals", International Journal of Fatigue, Vol.27, pp. 177-187.

Hoffmann, M. and Seeger, T., 1985, "A Generalized Method for Estimating Multiaxial Elastic-Plastic Notch Stresses and Strains, Part 1: Theory", J. Eng. Materials & Technology, Vol.107, pp. 250-254.

Meggiolaro, M.A., Castro, J.T.P. and Miranda, A.C.O., 2007, "A Critical Review of Classical Multiaxial Fatigue Damage and Stress-Strain Models", submitted to the J. Braz. Soc. Mech. Sci. and Eng., ABCM.

Sines, G., 1959, "Behavior of Metals Under Complex Static and Alternating Stresses", in Metal Fatigue, pp.145-169, McGraw-Hill.

Smith, R.N., Watson, P. and Topper, T.H., 1970, "A Stress-Strain Parameter for the Fatigue of Metals", J. of Materials, Vol.5, No. 4, pp.767-778.

Socie, D.F. and Marquis, G.B., 1999, "Multiaxial Fatigue", SAE International.

Zouain, N., Mamiya, E.N. and Comes, F., 2006, "Using enclosing ellipsoids in multiaxial fatigue strength criteria", European Journal of Mechanics - A, Solids, Vol.25, pp. 51-71.

9. RESPONSIBILITY NOTICE

The authors are the only responsible for the printed material included in this paper.